Surface & Coatings Technology 202 (2008) 4980–4985

Contents lists available at ScienceDirect

Surface & Coatings Technology

journal homepage: www.elsevier.com/locate/surfcoat

Microstructural and photocatalytic properties distribution of TiO_2 coatings reactively sputtered as a function of the substrate position relatively to the Ti target

E. Aubry [a,b,*], P. Miska [c], L. Gigleux [a], A. Mézin [a], V. Demange [a], A. Billard [d]

[a] Laboratoire de Science et Génie des Surfaces (UMR 7570 CNRS), Nancy Université, Ecole des Mines, Parc de Saurupt, CS 14234, 54042 Nancy cedex, France
[b] Femto-ST, Université de Franche-Comté, CNRS, ENSMM, UTBM, 26 Chemin de l'Epitaphe, 25030 Besançon cedex, France
[c] Laboratoire de Physique des Matériaux (UMR 7556 CNRS), Nancy-Université, Université Henri Poincaré, Nancy I, B. P. 239, 54506 Vandœuvre-lès-Nancy cedex, France
[d] Laboratoire d'Etudes et de Recherche sur les Matériaux, les Procédés et les Surfaces (LERMPS-UTBM), site de Montbéliard, 2 Place Tharradin, 25210 Montbéliard, France

ARTICLE INFO

Article history:
Received 6 February 2008
Accepted in revised form 28 April 2008
Available online 13 May 2008

Keywords:
Sputtering
TiO_2
Photocatalysis
Porous
Stress
High pressure
Substrates position

ABSTRACT

Amorphous and porous TiO_2 coatings were deposited by reactive magnetron sputtering at high pressure (3.4 Pa) on cold soda-lime glass placed at different positions relatively to the magnetron target, which corresponds to different impingement angles and target-to-substrate distances. The as-deposited coatings were heated at 450 °C under ambient air to crystallise into the photoactive anatase phase. The structural analyses combined with AFM experiments have shown a reduction of the crystallites and the lateral grain size with the removal of the substrate from the target axis inducing a specific area rise. Moreover, the stress state is all the less as compressive as the substrates are far away from the target. As a result, the photocatalytic properties are improved with the decrease of the incidence angle and with the target-to-substrate distance rise.

1. Introduction

The overall process of the heterogeneous photocatalysis can be decomposed into several steps, whose mechanisms were assigned to the physicochemical properties of the catalyst material [1]. Among these ones, we can quote the reactants absorption, the photocarrier generation and diffusion toward the surface. These properties depend strongly on the synthesis process. The sputtering method presents some advantages because varied properties can be obtained easily, which explains the numerous applications of the sputtered films, especially in the photocatalysis area with the development of supported anatase TiO_2 coatings. Many studies deal with the influence of the main deposition parameters *i.e.* the temperature effect [2–4], the oxygen partial pressure [5,6] and the total pressure [6–11] on the photocatalytic activity of titanium dioxide. These studies underline that an optimal pressure around 3 Pa and a *post*-annealing treatment seem to be favourable to the photocatalytic activity. In our knowledge, no article deals with the influence of the substrates position relatively to the target axis on the physicochemical properties of titanium dioxide coatings. However some studies have already proved theoretically [12] and experimentally the influence of the substrate position on the composition of co-sputtered coatings [13] or on the electrical or electrochemical properties of conductive oxide [14,15]. In this paper, the evolution of the TiO_2 coating properties simultaneously deposited has been studied according to the substrate position. First, the distribution of the microstructural properties, the morphology and surface topography with the substrate position relatively to the target, *i.e.* as a function of the incident vapour flux angle will be underlined. Then, these variations in terms of their influence on the stress state and the photocatalytic properties of the coatings will be discussed.

2. Experimental details

2.1. Film preparation

TiO_2 photocatalyst coatings about 1 μm-thick were deposited on cold soda-lime glass by reactive sputtering at high pressure. The experimental details of the deposition chamber are detailed elsewhere [16]. The dimensions of the glass substrate are $25 \times 75 \times 1$ mm^3. In order to prevent the diffusion of the alkali elements from the glass substrate, a SiN_x diffusion barrier was pre-sputtered [16]. The thickness of the SiN_x diffusion barrier is fixed at 1000 nm. Three SiN_x/glass substrates were placed on a rotating substrate-holder at different positions relatively to the axis, which corresponds to different incident angles α of the impinging particles and target-to-substrate distances D_{t-s} (Fig. 1).

* Corresponding author. Femto-ST, Université de Franche-Comté, CNRS, ENSMM, UTBM, 26 Chemin de l'Epitaphe, 25030 Besançon cedex, France.
E-mail address: eric.aubry@ens2m.fr (E. Aubry).

0257-8972/$ – see front matter © 2008 Elsevier B.V. All rights reserved.
doi:10.1016/j.surfcoat.2008.04.097

Increasing the distance from the target axis (toward the centre of the substrate-holder) decreases α and increases D_{t-s}. The position of each substrate is identified by the incidence angle associated to the centre of the sample. The rotation of the substrate-holder leads to an enhancement of the thickness homogeneity. Nevertheless, the substrate-holder rotation induces a fluctuation of the parameters α and D_{t-s} for a considered area. Indeed, the centre of the substrate-holder receives a continuous flux with constant incidence and kinetic energy, inversely proportional to D_{t-s}. On the contrary, the external ring area of the substrate-holder is alternatively submitted to a flux either energetic when the substrate passes next to the target ($\alpha \rightarrow 90°$) or practically thermalised with the displacement of the substrate far from the target ($\alpha \rightarrow 0°$) [17]. As a consequence, the coating is built from a succession of various fluxes. However, the majority of the coating is formed when the substrate passes next to the target, *i.e.* with a high kinetic energy of the impinged particles and a high incidence angle. For the stress measurements, Si beams substrates were used. Their dimensions were $5 \times 50 \times 0.38$ mm^3. The preparation conditions for this study are summarized in Table 1. The ratio of oxygen partial pressure to total pressure PO_2/P_t was fixed at 10% for all the experiments. The as-deposited coatings are amorphous. In consequence, the TiO_2/SiN_x/glass multi-coatings and TiO_2/Si system were *post*-heated at 450 °C under ambient air in order to crystallise the photoactive anatase phase.

Table 1
Deposition parameters of the TiO_2 sputtered on various substrates (SiN_x/glass and Si)

Substrates	SiN_x barrier thickness (nm)	Incidence angle α (°)	Target-to-substrate distance D_{t-s} (mm)	Working pressure P_t (Pa)	Intensity I (A)	Voltage V (V)
Glass	1000	75	56.9	3.36±0.02	0.5	491±12
Glass	1000	66	60.0	3.36±0.02	0.5	491±12
Glass	1000	48	74.0	3.36±0.02	0.5	491±12
Si	–	85	55.2	3.34±0.01	0.5	501±12
Si	–	70	58.5	3.34±0.01	0.5	501±12
Si	–	58	64.8	3.34±0.01	0.5	501±12
Si	–	48	74.0	3.34±0.01	0.5	501±12

2.2. Film characterization

The structural properties were investigated by X-ray diffraction in Bragg–Brentano configuration using a Co K_α radiation. Silicon powder was dispersed on the coating surface in order to calibrate the diffractograms. The surface and cross section morphologies were investigated with a Philips XL30 SFEG scanning electron microscope. The lateral grain size estimation was performed using atomic force microscopy Dimension 3100 in non-contact mode. The TiO_2 surface area

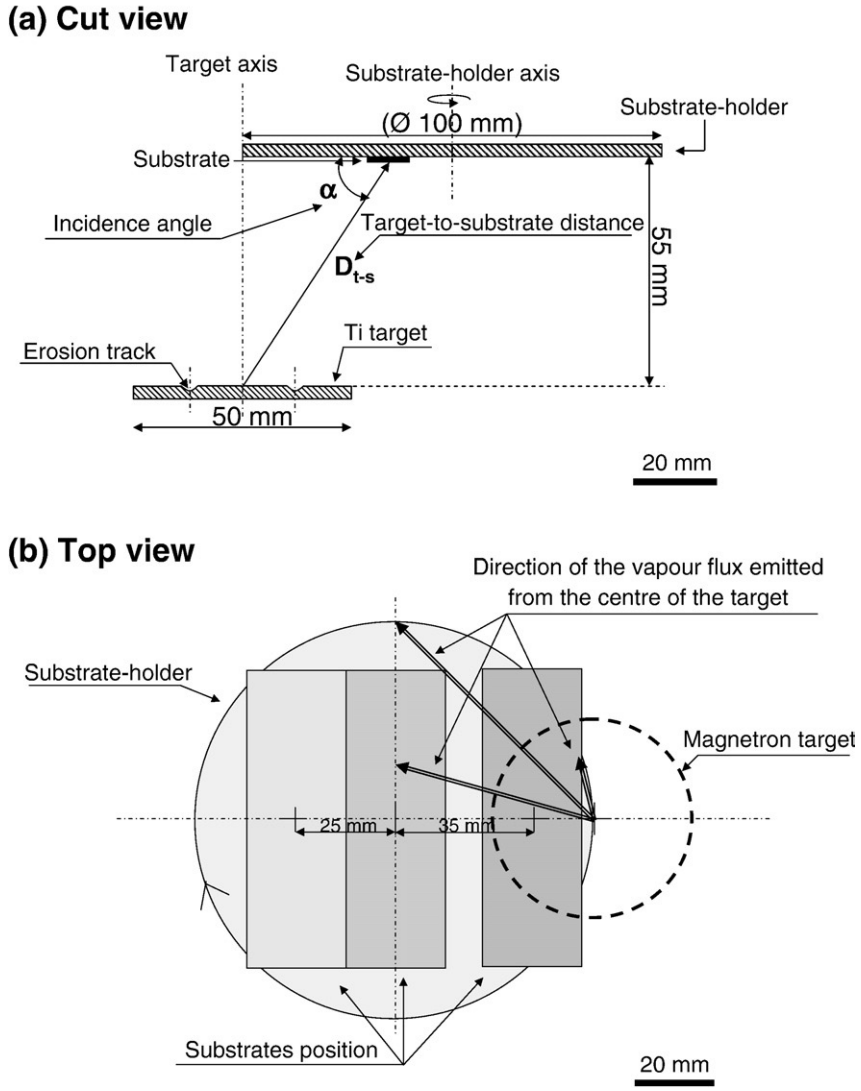

Fig. 1. Schematic representation of the experimental device : (a) cut view and (b) top view. The incidence angle α is defined by the lower angle between the surface of the substrate and the direction of the vapour flux emitted from the centre of the target.

was calculated by considering the AFM micrograph surfaces like triangles assembly whose peaks are defined by the (x, y, z) coordinates. So we can estimate the apparent surface area in adding the triangle area. These calculations were performed thanks to the WsXM software using $1 \times 1\ \mu m^2$ micrograph dimensions.

The in-plane stress was estimated from the simplified Stoney's formula by measuring the resulting curvature radii of the Si beams:

$$\sigma_f = \frac{E_s h_s^2}{6R(1-\upsilon_s)h_f} \quad (1)$$

where E_s, υ_s, h_s are respectively, the Young modulus, the Poisson coefficient and the substrate thickness, h_f, the coating thickness and R, the curvature radius. The simplification criteria are respected [18]. The beams are placed at different positions along the substrate-holder with particular incident angles (Fig. 1 and Table 1). The TiO_2 coating thickness was measured using the step method with a Talisurf profilometer. The crack density was evaluated statistically by counting the number of cracks by unitary length from MEB surface micrographs.

Finally, the photocatalytic activity of TiO_2 coatings was assessed by following the Orange II dye absorbance for 2 h by means of an experimental setup whose principle is based on that described in a previous article [16]. The photocatalytic activity is expressed in terms of apparent rate constant K' in min^{-1}. It must finally be mentioned that the chemical, structural and morphological analyses were carried out in a localised area in the centre of the samples whereas the photocatalytic activity measurements were determined on the overall sample ($75 \times 25\ mm^2$).

3. Results

3.1. Structural and microstructural properties

The structure of the annealed TiO_2 coatings synthesised on SiN_x/glass substrates placed at different positions relatively to the substrate-holder is presented in Fig. 2. All the coatings crystallise under the anatase structure (00-021-1272 JCPDS card number) whatever the sample position along the substrate-holder. The XRD patterns reveal a [001] preferential orientation meaning that a majority of (001) planes are parallel to the surface whereas the (200) planes are normal. The full width at half maximum (FWHM) of the (004) reflection of the TiO_2 coatings synthesised at different positions is presented in Fig. 3. The FWHM falls when the incidence angle rises, which means that the crystallite size grows in the direction perpendicular to the surface all the more as the incidence angle tends to 90°. The texture effect allows the determination of the cell parameters using the following formulae for a tetragonal symmetry:

$$c = 4 \times d_{004} \quad (2)$$

$$a = \frac{d_{101} \times 4d_{004}}{\sqrt{16d_{004}^2 - d_{101}^2}} \quad (3)$$

Fig. 4 shows the cell parameters of the TiO_2 coatings for different incidence angles. According to their [001] texture, the comparison of the a cell parameter with its theoretical value reflects the strain parallel to the surface and thus the stress state following Hooke's law. Both parameters are lower than the theoretical ones (a=0.3785 nm and c=0.9514 nm from the JCPDS 00-021-1272 card number), indicating that the coatings are submitted to compressive stress. Moreover the cell parameters decrease with increasing the incidence angle, suggesting that the compressive stress is more important at normal incidence, which corroborates previous studies [19–21].

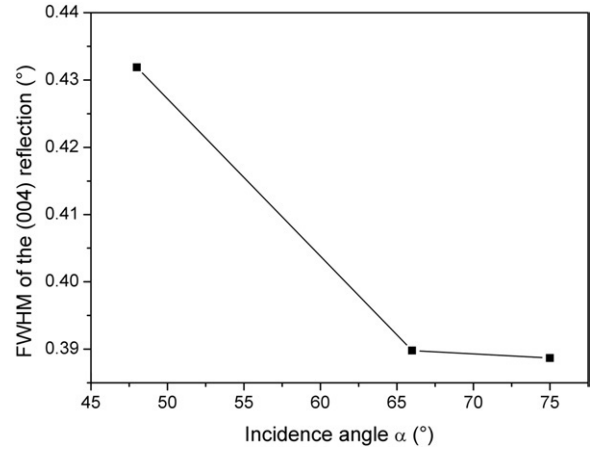

Fig. 3. Full Width at Half Maximum of the (004) reflection for different incidence angles.

3.2. Morphology

The evolution of the coatings morphology with the incidence angle can be observed on SEM top surface and brittle-fracture cross section (see Fig. 5). Accordingly with the high working pressure and the low substrate temperature, the coatings are constituted by columns separated by void

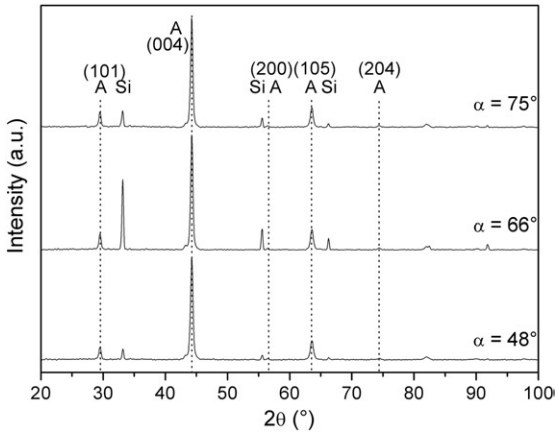

Fig. 2. X-ray diffractograms of the annealed TiO_2 coatings for different incidence angles (A: anatase).

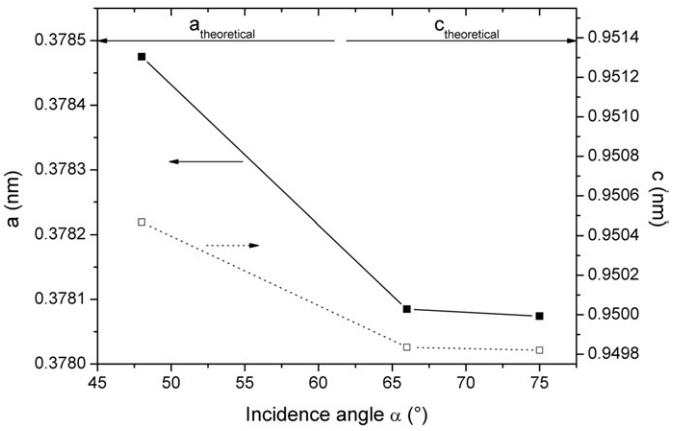

Fig. 4. Evolution of the anatase cell parameters with the incidence angle.

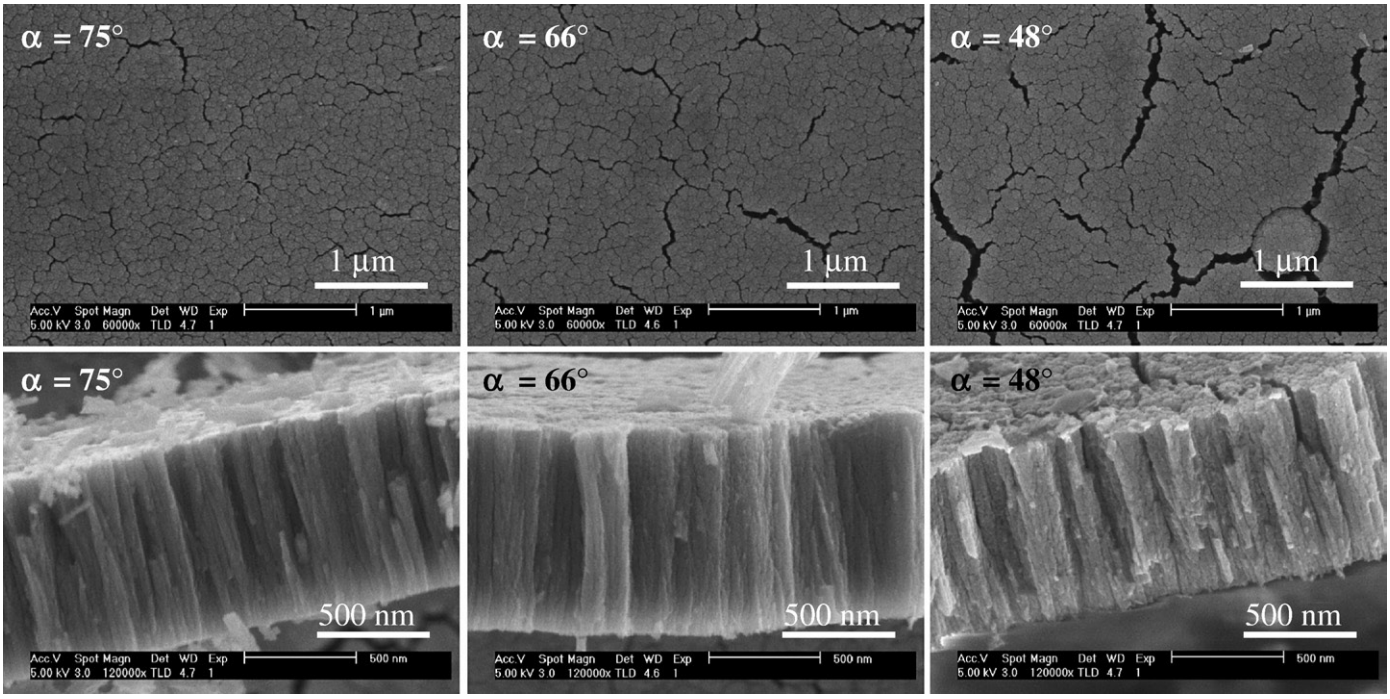

Fig. 5. SEM micrographs of the top surface and cross-section of the annealed TiO_2 films elaborated at different incidence angles.

boundaries. The surface and the columns seem to be rougher at low incidence. SEM micrographs show that the TiO_2 films present stronger and wider cracks for the low impingement angle. The highest cracking at low incidence angle could explain the reduction of the magnitude of the compressive stress [21]. The top-surface morphology observation has also been performed by atomic force microscopy. The corresponding micrographs at different magnifications are presented in Fig. 6. We can distinguish that each column is composed by nanometric grains separated by porosities [22]. The lateral size of these particles, presented in Fig. 7 as a function of the incidence angle α, indicates that this size increases with the incidence angle. From the XRD and AFM results, we conclude that the growth with an oblique impingement induces a reduction of the grain volume. As a consequence, the surface area presented in Fig. 7 undergoes a strong increase with the reduction of the grain size.

3.3. Internal stress in TiO_2 films

Fig. 8 represents the evolution of the in-plane stress in TiO_2 deposited on Si beams before (solid line) and after annealed at 450 °C (dashed line). The stress state in the amorphous as-deposited films is characteristic of the intrinsic stress. This stress is in tensile, according to the high pressure and the columnar morphology [23,24]. At α=70°, we can note compressive stress apparition due to the bombardment

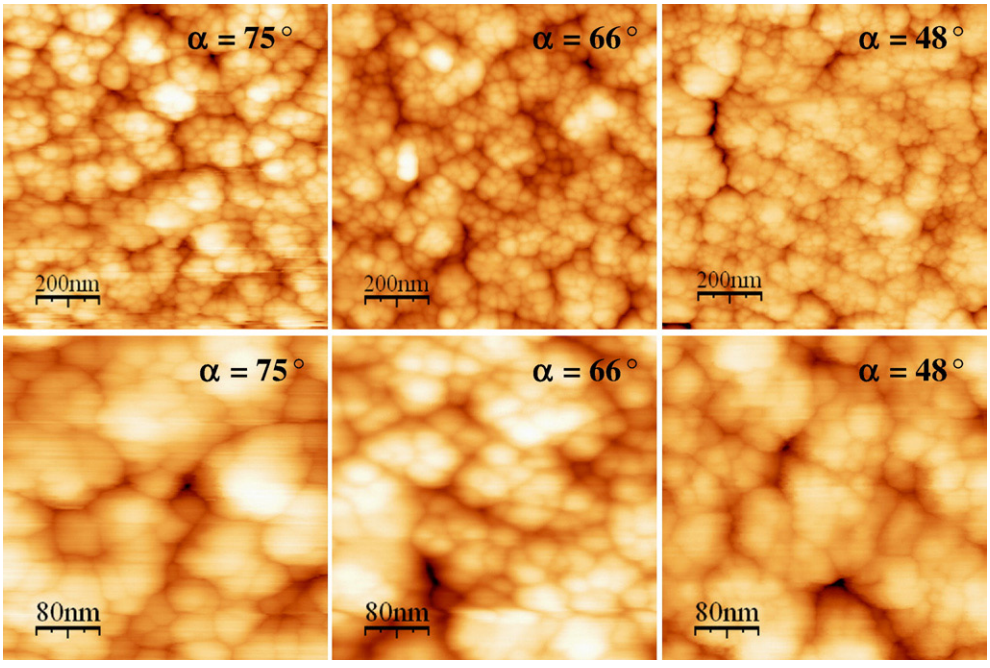

Fig. 6. AFM micrographs of the annealed TiO_2 coatings as a function of the incidence angle.

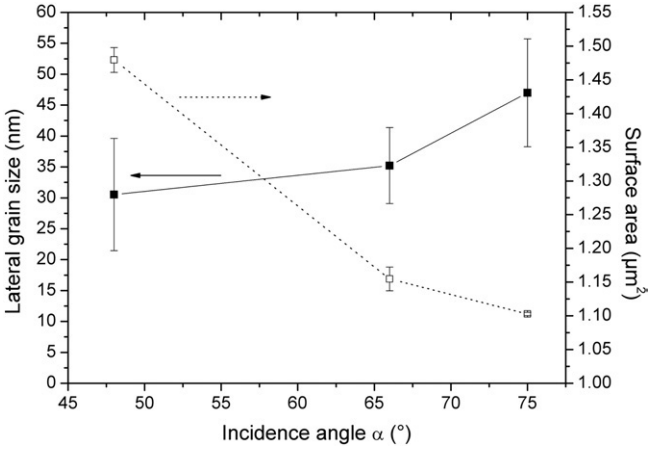

Fig. 7. Evolution of the lateral grain size and of the developed surface area estimated from 1×1 μm² AFM micrographs of the annealed TiO_2 coatings as a function of the incidence angle.

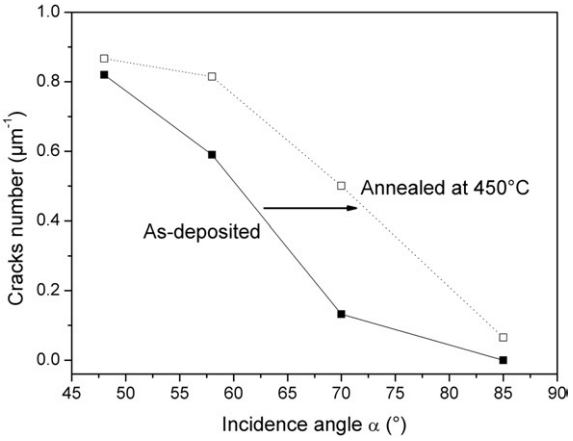

Fig. 9. Cracks number per length unity in the TiO_2 films synthesised on Si beams at different incidence angles before and after annealing at 450 °C.

by energetic particles emitted from the erosion track of the target. The crystallisation treatment induces a shift of the biaxial stress toward negative values with a magnitude of 100–200 MPa, synonym of compressive stress. The shape of the curve is quite conserved and displaced towards compressive values, which should indicate that the thermal stress is practically equal whatever the substrate position. The discrepancy between the thermal expansion coefficients of the substrate and the coating is assumed to generate thermal stress, during the *post*-annealing treatment, defined by [23]:

$$\sigma_{th} = \frac{E_f(\alpha_f - \alpha_s)}{(1-\nu_f)}\Delta T \quad (4)$$

where E_f, ν_f, α_f and α_s are respectively the Young modulus (290 GPa), the Poisson coefficient (0.28), the thermal expansion coefficients of the coating ($7.6\cdot10^{-6}$ K^{-1}) and of the Si substrate ($3\cdot10^{-6}$ K^{-1}) [25]. ΔT is the temperature discrepancy between room temperature and the annealing temperature. As a consequence, during the heating, the coating is submitted to compressive stress whereas the cooling induces tensile stress. Moreover the anatase crystallisation creates tensile stress due to the volume reduction. However, the resulting stress of the films after heat treatment is compressive. This phenomenon could be explained by the consumption of lattice defects and/or by the porous character of the TiO_2 film. Indeed, the water adsorption by capillarity along the columns should disturb the Van de Waals links across the grain boundaries leading to a stress magnitude decrease [26]. Nevertheless, these results are in agreement with the anatase cell parameters. This hypothesis is supported by other results which are not presented in this paper, *i.e.* for dense TiO_2 films elaborated at low pressure, the crystallisation treatment induces tensile stress according to the volume reduction and the thermal expansion coefficient discrepancy of the substrate and the coating [27].

The low values of tensile stress in the as-deposited coatings could result from their amorphous character [24] and by the relaxation phenomenon produced by the transversal cracking, as shown by Fig. 9. Before annealing (solid line) the cracks number increases at low incidence angles, demonstrating that the tensile intrinsic stress is more important in the coating elaborated at low incidence angle. After the annealing of coatings deposited for intermediate incidence angles, when the accumulation of tensile stress (intrinsic and crystallisation) becomes sufficient, the transversal cracking produces and shifts the cracks number curve toward intermediate angles (dashed line).

3.4. Photocatalytic properties

The photocatalytic activity has been determined by following the degradation of the Orange II *vs* time under irradiation using a Xe lamp. Fig. 10 reveals the evolution of the apparent rate constant *K'* of the TiO_2 coatings elaborated at different incidence angles. A slight increase of the constant *K'* of about 20% is observed with decreasing the

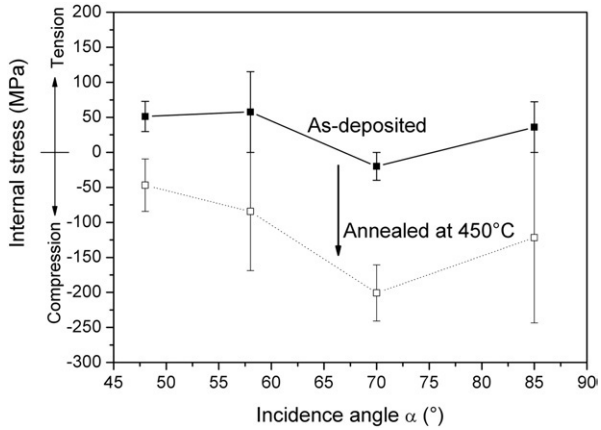

Fig. 8. Internal stress of the TiO_2 coatings synthesised at different incidence angles on Si beams before and after annealing at 450 °C.

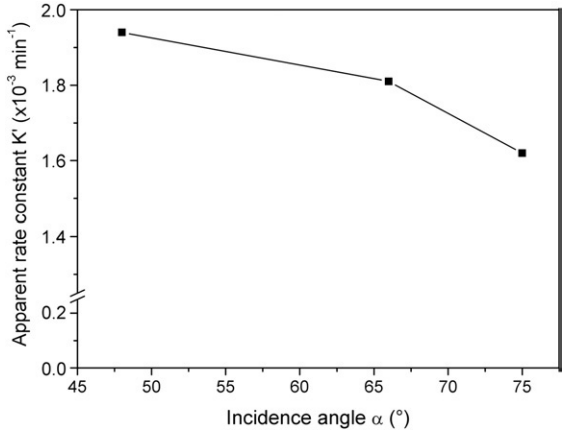

Fig. 10. Apparent rate constant of the annealed TiO_2 coatings synthesised on SiN_x/glass substrates in function of the incidence angle.

incidence angle. This evolution is lower than that expected owing to the increase of about 40% of the developed surface area with decreasing the impingement angle α from 48° to 75° (see Fig. 7). Such a lower evolution of the photocatalytic activity compared to the increase of the developed surface area has to be related to the rather large area of the glass substrate owing to the deposition reactor dimension, *e.g.* the glass slide located at α=48° (centre of the glass slide) corresponds to real impingement angles α distributed between 32° (closest edge of the glass slide) and 80° (farthest edge of the glass slide). As a consequence, the developed area of the coating surface over the whole glass slide support is lower than that measured for the reference angle at the centre of the glass slide. This clearly explains the lower photocatalytic activity enhancement than that expected from the specific area increase resulting from the measurements localised at the centre of the samples.

4. Discussion

Three SiN_x/glass substrates placed at different positions on a rotating substrate-holder have been simultaneously covered by a TiO_2 film. The as-deposited amorphous coatings always present tensile stresses, conformably with the rather high deposition pressure [28]. A model proposed by Hoffman argues that tensile stress is a natural consequence of interactions at the grains boundaries [24]. The attraction between neighbour grains throughout the void space creates a localised tensile stress. Moreover the transversal cracking becomes more important at low incidence angle, meaning that the tensile stress is higher. A low incidence angle implies a high D_{t-s}, hence a strong loss of the kinetic energy of the impinging particles which condense without diffusion on the cold substrate. The coatings are amorphous and columnar with a porosity *intra* and *extra* columnar all the most than the incidence angle is low. During the annealing at 450 °C, the anatase structure crystallises with a [001] preferential orientation. The TiO_2 coatings synthesised at low incidence angle with a low kinetic energy of the impinging particles present a lower grain volume attributed to the more important porosity. It results in an increase of the developed surface area. Besides, the heat treatment under air shifts the stress towards compressive state and new cracks appear due to the crystallisation. The stress relaxation associated with the cracks development is then more pronounced for the lower incidence angle, *i.e.* for the strongest tensile stress. From this consideration, the photocatalytic activity increase at low incidence angle should be attributed to the surface area development (rising of the adsorption sites) and/or to the relaxation (decreasing of the number of recombination centres).

5. Conclusion

In this article, we have demonstrated that TiO_2 films present a properties distribution as a function of their position on a rotating substrate-holder. Due to lower energy and incidence angle with increasing the distance between the substrate and the axis of the Ti target, the films acquire a more developed surface and become more relaxed, which is favourable for their photocatalytic activity. Despite the rotation of the substrate-holder to improve the thickness homogeneity, the coatings developed a gradient of the nanostructural properties even at high pressure. The understanding of such a phenomenon participates to the enhancement of the coating reproducibility. Moreover we have shown that annealing treatments performed to crystallise the amorphous coating under the desired anatase phase can yield compressive stress despite their initial extensive stress and that occurred during the coating crystallisation. This phenomenon should be attributed to the absorption of water vapour in nano size intercolumnar porosity of the coatings deposited at high pressure.

References

[1] J.-M. Herrmann, Catal. Today 53 (1999) 115.
[2] S.K. Zheng, T.M. Wang, G. Xiang, C. Wang, Vacuum 62 (2001) 361.
[3] S. Takeda, S. Suzuki, H. Odaka, H. Hosono, Thin Solid Films 392 (2001) 338.
[4] H. Wang, T. Wang, P. Xu, J. Mater. Sci. Mater. Electron. 9 (1998) 327.
[5] B. Liu, X. Zhao, Q. Zhao, C. Li, X. He, Mater. Chem. Phys. 90 (2005) 207.
[6] P. Zeman, S. Takabayashi, Surf. Coat. Technol. 153 (2002) 93.
[7] M. Yamagishi, S. Kuriki, P.K. Song, Y. Shigesato, Thin Solid Films 442 (2003) 227.
[8] W. Zhang, Y. Li, S. Zhu, F. Wang, Surf. Coat. Technol. 182 (2004) 192.
[9] K. Eufinger, E.N. Janssen, H. Poelman, D. Poelman, R. De Gryse, G.B. Marin, Thin Solid Films 515 (2006) 425.
[10] D. Noguchi, Y. Kawamata, T. Nagatomo, Jpn. J. Appl. Phys. 43 (2004) 4351.
[11] P. Zeman, S. Takabayashi, Thin Solid Films 433 (2003) 57.
[12] A. Billard, C. Frantz, Surf. Coat. Technol. 59 (1993) 41.
[13] O. Bouaziz, A. Billard, Surf. Coat. Technol. 201 (2007) 7007.
[14] D. Horwat, J.F. Pierson, A. Billard, Surf. Coat. Technol. 201 (2007) 7060.
[15] D. Horwat, A. Billard, Thin Solid Films 515 (2007) 5444.
[16] E. Aubry, M.N. Ghazzal, V. Demange, N. Chaoui, D. Robert, A. Billard, Surf. Coat. Technol. 201 (2007) 7706.
[17] A. Billard, M. Foos, C. Frantz, M. Gantois, Surf. Coat. Technol. 43–44 (1990) 521.
[18] A. Mézin, Surf. Coat. Technol. 200 (2006) 5259.
[19] J.F. Pierson, A. Billard, T. Belmonte, H. Michel, C. Frantz, Thin Solid Films 347 (1999) 78.
[20] F. Lapostolle, F. Perry, A. Billard, Surf. Coat. Technol. 201 (2006) 2633.
[21] F. Lapostolle, A. Billard, J. von Stebut, Surf. Coat. Technol. 135 (2000) 1.
[22] R. Messier, A.P. Giri, R.A. Roy, J. Vac. Sci. Technol. A 2 (1984) 500.
[23] J.A. Thornton, D.W. Hoffman, Thin Solid Films, 171 (1989) 5.
[24] R.W. Hoffman, Thin Solid Films 34 (1976) 185.
[25] N. Jagtap, M. Bhagwat, P. Awati, V. Ramaswamy, Thermochim. Acta 427 (2005) 37.
[26] G. Atanassov, J. Turlo, J.K. Fu, Y.S. Dai, Thin Solid Films 342 (1999) 83.
[27] E. Aubry, PhD thesis (in French), Institut National Polytechnique de Lorraine, Nancy, France, 2007, http://www.scd.inpl-nancy.fr/theses/2007_AUBRY_E.pdf.
[28] F. Sanchette, A. Billard, Surf. Coat. Technol. 142–144 (2001) 218.